Increasing Accuracy of Winding Insulation State Indicator of Three Phase Inverter-fed Machines using Two Current Sensors only

C. Zoeller, Th. Winter, Th. M. Wolbank
Institute of Energy Systems and Electrical Drives
Vienna University of Technology
Vienna, Austria
thomas.wolbank@tuwien.ac.at

M.A.Vogelsberger
GSC/PPC-Drives VI
Bombardier Transportation Austria GmbH
Vienna, Austria
markus.vogelsberger@at.transport.bombardier.com

Abstract— **In modern traction drives the application of monitoring systems is growing to ensure continuous operability. Because of the voltage source inverters (VSI) and the high steep voltage change (*dv/dt*), increased stress of the winding insulation exist. Stator insulation faults are common reasons for a machine breakdown. Insulation health state can be examined by evaluating the transient reaction to a voltage step excitation. Using the inverter as a source of excitation, it is possible to perform an insulation test by evaluating the resulting transient current sensor signals. The trace of the machines transient current reaction depends on the state of the winding insulation system. If insulation degradation occurs the parameters like the parasitic winding capacitances are changing and influencing the trace of the ringing. Normally, for a three phase AC machine the state of every phase is analyzed with the corresponding current sensor. However, regarding the economic issue, the usage of system resources and additional components is restricted. With the proposed method the evaluation of the stator insulation condition is possible only with two current sensors. The state of the phase without a sensor can be analyzed by a special excitation sequence without significant deterioration of sensitivity compared to the results if a sensor is available. Because the transient reaction of non-excited phases is very small, enhanced signal preprocessing is required to prevent sensitivity losses.**

***Index Terms*--AC motor drives, Insulation monitoring, Fault detection, Induction machines, Insulation degradation, Switching transients, Trigger detection**

I. Introduction

The demand of monitoring systems to prevent breakdowns of modern traction drive systems is continuously increasing. The drives offer high dynamic performance and are used for example in safety-critical applications as well as in public and cargo transportation systems. Availability and reliability are key factors to consider safe and efficient operation of the drive system. With 35%, stator related faults are specified as the second most common faults, causing a machine outage, see [1] and [2].

The work to this investigation was supported by the Austrian Research Promotion Agency (FFG).

Furthermore about 70% of these stator faults are based on a failure of the insulation system. Insulation condition monitoring assists to ensure a detection of insulation degradation in an early stage. A degraded insulation at first leads to a turn to turn, phase to phase and finally to severe ground faults as described in [3].

Different stresses like electrical, thermal, thermo-mechanical, mechanical and environmental are stated as responsible causes for a reduced insulation lifetime [4]. It is common that the process of insulation degradation is proceeding very slowly, sometimes even over decades. In [5] the effect of thermal-electrical aging for high operation time and a high number of thermal-mechanical aging cycles on the stator bars are analyzed. The results of experiments on simple epoxy resin coil specimens, representing a stator segment, show that the capacitance of the specimen has changed over time and with the number of aging cycles. In [6] a change in the turn-turn capacitance of a form-wound coil after stress through thermal cycles is detectable. The capacitance is in all cases considered as the dominant parameter for insulation health state evaluation.

In modern traction drives the insulation additional suffers through voltage source inverter (VSI) and the fast switching, causing steep voltage steps (*dv/dt*). In combination with improper cabling, an overvoltage of 2-4 DC-link voltage is possible [7].

With the proposed method in [8] insulation condition monitoring only based on the current sensors signals is shown. The method analyses the characteristics of the transient part of the current sensor response if a step voltage is applied. The same sensors are also needed for the control of the machine, thus no additional sensor hardware is necessary. Depending on the insulation condition, changes in the transient signal ringing of the current sensors responses occur. Every phase is analyzed with the corresponding current sensor. Regarding the economic view a reduction of the system components save costs and one current sensor is omitted. This puts additional challenges to the insulation monitoring method. The

sensitivity of the non-directly excited phases is not high enough to detect small insulation degradations. A reconstruction of the missing current signal from the assumption that the sum of all phase currents is zero is only possible in the low frequency range and not suitable for the transient parts. Before the characteristics of the transients can be analyzed, a signal preprocessing is necessary to prevent external influences, e.g. jitter. To analyze the effect of jitter in the inverter output waveform, different trigger detection algorithms were implemented and developed with respect to hardware implementation.
The measurements are conducted on a test stand with a special type 1.4 MW induction machine.

II. General Aspects of the Proposed Method

In theory the insulation degradation is always linked with a capacitive change, as mentioned in the section before. Thus, the proposed method analyses the characteristics of such changes in the winding system. This is realized with a special 1.4MW induction machine using tappings at specific positions of the winding. In Fig. 1 a scheme of the machine and the existing parasitic capacitances $C_{ph\text{-}ph}$, $C_{ph\text{-}gnd}$, C_{ph}, $C_{m\text{-}gnd}$ is depicted.

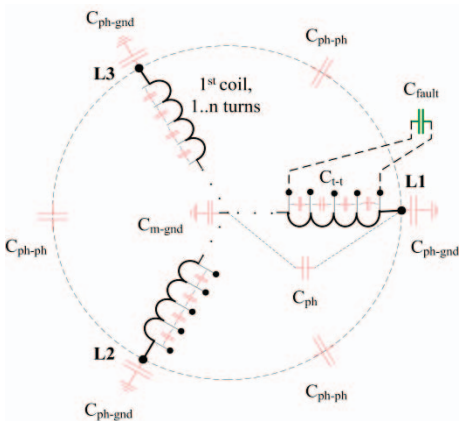

Fig. 1 Schematic view of the complex system inverter, cabling and machine with parasitic capacitances.

In addition to the always existing parasitic elements, e.g. phase to phase $C_{Ph\text{-}Ph}$, phase to ground $C_{Ph\text{-}Gnd}$ and turn to turn $C_{t\text{-}t}$, the external placed fault capacitor C_{Fault} is also depicted. The basic insulation health state monitoring method with three sensors is based on analysis of the transient current reaction to a step voltage excitation in every strand separately. With the inverter, every phase is excited, e.g. with a switching transition from an inactive to an active inverter output state. The fast rising voltage steps in combination with the improper terminated transmission lines from the inverter to the machine cause transient overvoltage on the end of the line. This ringing is also observable in the current sensor response. In

Fig. 2 the current response for a healthy machine without additional fault capacitor parallel the winding (solid black trace), to a pulse excitation from lower short circuit to a positive switching state in the corresponding phase is shown. This measurement serves as a reference and further measurements with different fault scenarios are compared to this result. The solid blue trace represents the current response if a 15nF capacitor is placed parallel the whole phase L1. Both traces are recorded with a Tektronix current probe. The transient part is visible within the first 20µs. A clear deviation between the healthy (reference) and the emulated insulation degradation measurement is visible. Omitting one phase current sensor leads to a lack of information of the insulation state of one phase. A simple substitution of the missing transient current reaction by using the sum of the two other currents is not helpful and is only valid for low frequencies. The sum of the transient current signal part is different from zero through e.g. the appearance of displacement currents.

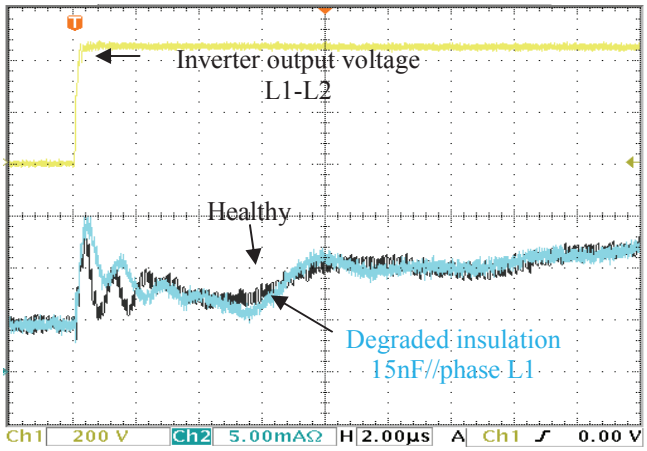

Fig. 2 Resulting phase current signal to voltage pulse excitation in the corresponding phase.

Using this composite signal does not deliver satisfactory results. Furthermore, the transient current reaction in the non-excited phases is very small and hardly influenced by a change of the phase capacitance, as depicted in Fig. 3 with the same scenario used in Fig. 2 (15nF//phaseL1).

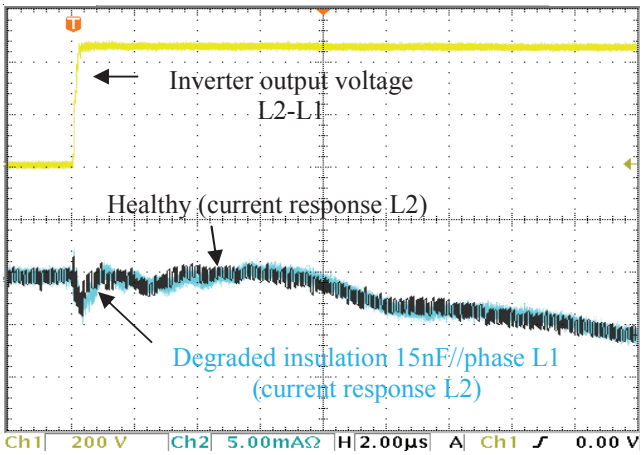

Fig. 3 Current response of phase L2 for pulse excitation in phase L1. Black trace: healthy machine; blue trace: emulated insulation degradation with 15nF parallel whole phase L1.

The voltage step excitation is again applied to phase L1. With 15nF parallel whole phase L1 the solid blue trace hardly shows any visible deviations compared to the healthy machine

state (solid black trace). Despite the phase with degraded insulation (L1) is directly excited, a change in the machine state is hardly observable in the non-excited current reaction (L2). Therefore, a new excitation and signal processing method has been developed, which is described in a later section of this paper.

A. Measurements and fundamentals of the method

The time signals of the current responses are transferred into frequency domain, using the Fast Fourier Transformation (FFT). Afterwards, the deviation is analyzed and an indicator is calculated to deliver information about the severity of the changes. Before the FFT is applied, a signal preprocessing is necessary to deliver exact results. The whole signal pre-processing chain starts with the accurate detection of the actual switching instant that is varying between different measurements through the inverter jitter. This is followed by the removal of the mean current derivative resulting from the applied voltage step, as well as a removal of the final signal offset. The mean derivative is removed to prevent influences of inherent machine asymmetries, e.g. slotting. The estimated signal start point also influences the mean derivative calculation. A high fluctuation of the start point, and as a consequence of the signal slope, leads to inaccuracies of the spectra concerning the lower frequency range. In Fig. 4 (upper figure) the current response of phase L1 if voltage step excitation of the same phase is applied is shown. Fig. 4 (lower figure) depicts the resulting signal after the signal preprocessing is done.

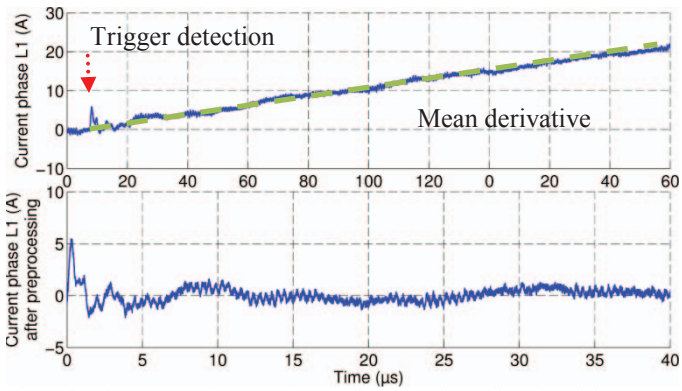

Fig. 4 Signal preprocessing steps (upper figure) and resulting signal (lower figure)

The traces represent the measurements on a machine with zero current and zero flux level, recorded with a standard industrial current sensor with a specified bandwidth of DC-150 kHz and a maximum di/dt of 50A/µs. To enable statistical analyses and improve the performance of the method, a high number of single measurements (at least 40) are carried out to represent one machine insulation state. The consecutive measurements are done with a real-time system and two FPGA modules (inverter controlling and measurement unit) with a 40MS/s ADC unit. The signal of Fig. 4 b) is transferred with the FFT into frequency domain for a healthy machine state and the faulty machine state emulated with 15nF placed in parallel to the whole phase L1. The results are shown in Fig. 5. The blue trace represents the mean of 40 spectra of the healthy machine. The green trace is the result of the mean of 40 spectra with emulated insulation degradation (15nF//1st coil phase L1). A change of the green trace with respect to the reference can be interpreted as insulation degradation. The dashed red trace depicts the square deviation between the two other traces. The observed frequency range is selected from 50 kHz to 500 kHz.

As the frequency range of interest is outside the specification of the current sensors, their signal accuracy is clearly reduced. However their transfer functions are still reproducible. The most noticeable change of the frequency spectrum due to the additional capacitor occurs in a very narrow range around 100 kHz to 200 kHz. The main deviation depends on the size and position of the capacitance, therefore the whole frequency range mentioned before is analyzed.

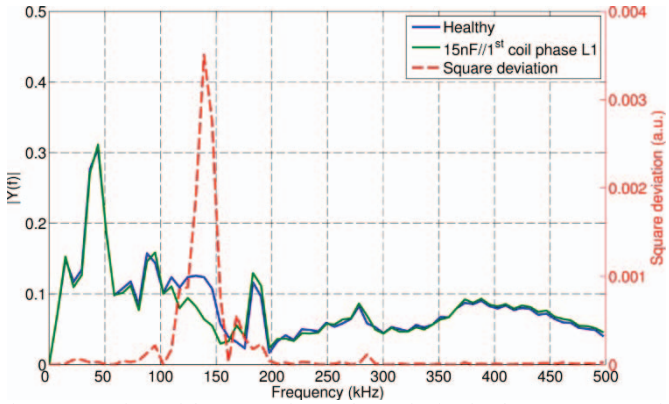

Fig. 5 Comparison of the spectra for a pulse excitation in phase L1 (measured phase L1)

Further, an indicator is introduced to assess the severity of the insulation degradation. The Root Mean Square Deviation (RMSD) calculated with the spectra of reference measurements and further measurements has been found to be a good indicator to express the severity of the insulation change. The indicator is denoted with ISI_2S (two sensors). With equation (1) the RMSD between two traces is calculated.

$$ISI_p = RMSD_p(x_1, x_2) = \sqrt{\frac{\sum_{i=1}^{n}\left(Y_{ref-sum,p}(f_i) - Y_{con,p}(f_i)\right)^2}{n}} \quad (1)$$

$$Y_{ref-sum,p} = \frac{\sum_{i=1}^{l}\left(\sum_{k=1}^{m}\frac{Y_{ref,p,k}}{m}\right)_i}{l};\ Y_{con,p} = \frac{\sum_{k=1}^{m} Y_{con,p,k}}{m}; \quad (2)$$

The index p identifies the investigated phase. The variables $Y_{ref\text{-}sum,p}$ and $Y_{con,p}$ represent the mean of the amplitude spectrum of at least one reference and of a later condition measurement respectively. The variable n depends on the time window length. To increase the accuracy, quantity of measurements for the mean in equation (2) is set to at least 33 measurements (Index m). The principle in detecting changes in the current response through repetitive measure procedures demands same conditions in every measurement. The reference signals are confirmed through several test measurements at a healthy machine state. Only after the reference signal can be verified the examination of changes

can be done. It is recommended to improve the signal processing method with a high number (l) of reference measurements taken at different time instants and to use the mean as base value $Y_{ref\text{-}sum,p}$ (Index l) for the comparison. With the correctly obtained reference and further measurements the comparison and observation of changes in the current response is possible.

B. *Omitting one current sensor*

Because of the economic reasons, one current sensor is omitted and hence costs can be reduced. As depicted with Fig. 3 the deviation between the healthy and faulty state is very small, if measured with the non-excited phases. The spectra show also hardly deviations. For this reason, a new method is proposed to detect also small changes with only two current sensors. The new method is based on comparison of different step excitations and current reactions of the non-excited phases. The new indicator serves as an enhancement of the normal ISI (three current sensors) to facilitate the omission of one current sensor and to observe the insulation condition of the non-measured phase. For the following explanation it is assumed, that no sensor in phase L1 is available. The new method uses four voltage step excitations, denoted I,II, and III, IV, as depicted in block "*4 step combination*".

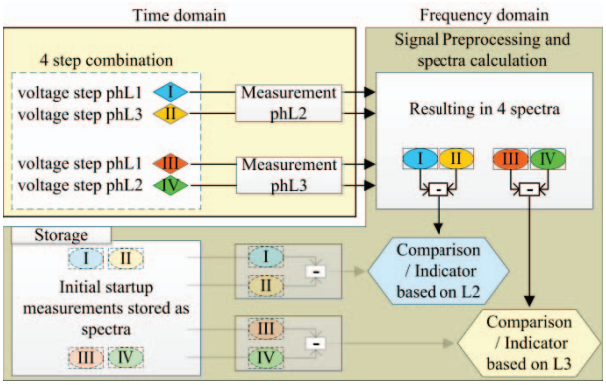

Fig. 6 Scheme of the two sensor method

First the measurements are done only with sensor phase L2 if two equivalent voltage steps (I,II), one in phase L1 and one in phase L3 are carried out. Comparing the two measurements, especially the spectra ("*Signal preprocessing and spectra calculation*" block of Fig. 6) gives an evidence for a possible asymmetry of phases L1 and L3. The procedure described above is repeated for excitation in phase L1, L2 and measurement in phase L3 (voltage steps III and IV). Thus, the measurement of the current reaction is always taken in the non-excited phase and the resulting spectra are used for the evaluation. The comparison of I and II respectively III and IV is done with the simple difference of the spectra. In case of an ideally symmetric machine, the spectra should be equal and the difference result to zero. In the next step the initial startup measurement from storage (see lower left part of Fig. 6) and the results of the difference spectra are compared to the results of an actual measurement. If insulation degradation occurs, a deviation in all calculated spectra is observable and the comparison to the stored data will indicate the severity. Again, an indicator based on the RMSD value was introduced to assess the severity of the insulation degradation. With equation (1) the RMSD between the difference of I and II for the healthy machine state and I and II for the faulty machine state is calculated. The same is done for difference of III and IV. This will result in an indicator based on measurements of L2 and another one based only on measurements with L3. The average of both is used to give an evidence of the state of the machine. In Fig. 7 the results for different fault scenarios and the corresponding ISI_2S values (two sensors) in comparison to the ISI (three sensors) are depicted. The values are scaled to a second reference measurement which is compared to the healthy measurement. As a consequence, a value of "1" on the vertical axes represents the detection limit.

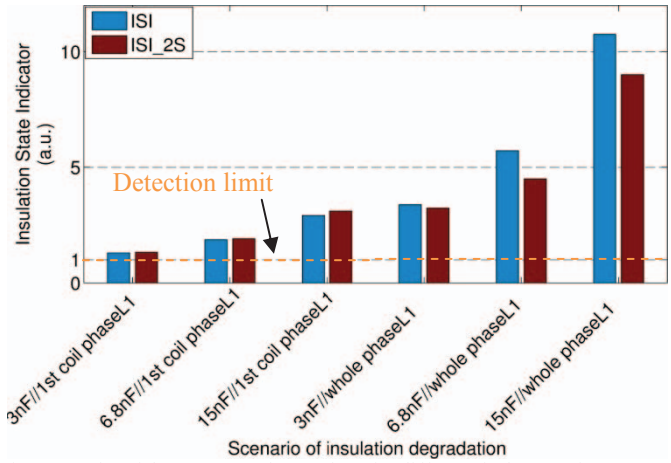

Fig. 7 Results of the ISI_2S and ISI values for different fault scenarios.

There is no significant deterioration of sensitivity if one single phase current sensor is omitted and all fault scenarios are detectable and indicates insulation degradation.

C. *Improvements in signal preprocessing*

Because of the first rising edge's low magnitude of the indirect measured current responses (see Fig. 3) the exact trigger (start point of the rising edge) is difficult to detect, especially at noisy data. The placement of a fixed start point is not recommended, particularly if jitter in the output waveform of the inverter exists. As is known, a shift of a time function has no effect on the magnitude spectra and only affects the phase, an inaccurate detection of the start point leads to deviations in the mean derivative calculation. Furthermore, if the start point is placed after the first ringing occurred, also the magnitude spectrum is influenced. Thus in the following, three different trigger detection algorithms are compared with respect to their detection accuracy, as well as their real time applicability.

- *Trigger detection based on differences*

This algorithm uses the principle of a steep rising edge at the beginning of the current response after a voltage step is applied. With a high sampling rate, the transient part is recorded with a resolution, high enough to compare a sequence of sample points with respect to the first rising edge of the oscillation on increasing values. The complete signal is analyzed in blocks with a length of seven consecutive sample

points. The difference of the adjacent points is calculated and at least four differences need to be higher than a specified threshold. The threshold depends on the ADC unit resolution and the signal to noise ratio (SNR). If the condition that four differences are higher than a threshold is met, the start point of the signal is set to the start index of the block. If the condition is not met, the whole block is shifted by one sample point. As the ADC unit is triggered before the voltage pulse is applied, a short period of the idle state before the switching transition is also recorded. To save calculation time, the beginning of the trigger detection process is set to a fixed configured index. Due to poor SNR, it is possible that no start point can be found and the trigger detection fails. In that case the start point of the signal is set to a default value. The properties of the algorithm are as follows:

- simple mathematic implementation
- many parameters have to be considered (start of trigger detection process, threshold for difference, quantity of difference higher than threshold, default value)
- no causal behavior, the whole signal has to be known, hardly suitable for online-implementation
- no reliable detection of the start point in case of noisy data

Fig. 8 depicts a histogram of the evaluated start points of 1500 single measurements. On the abscissa the indices, representing the determined start points of the current responses are depicted. With a sampling rate of 40MS/s, a sample point is recorded every 25 ns. The most detected starting point index is 155 and in a range of ±5 the majority of start points are determined. However, the distribution is spread from index values 150 to 170.

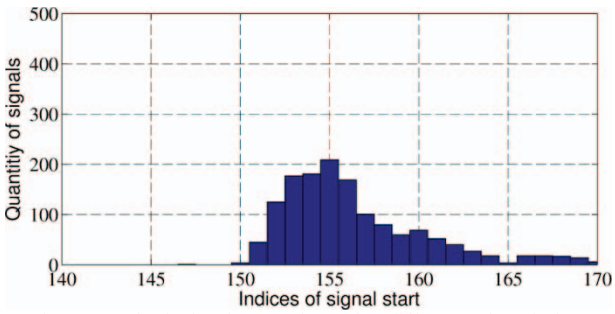

Fig. 8 Histogram of calculated start points using differences based trigger algorithm

➢ *Trigger calculation with cross-correlation function*

The same set of measurements is analyzed with another trigger detection algorithm. The detection of the signal start point now is calculated using the cross-correlation function. The basic idea is that the first recorded signal, especially the first few μs consisting the transient part, serves as the pattern for a comparison to all other measurements. The start point of the first signal is determined manually. The cross-correlation based on equation (3) is calculated for the first measurement y_m^* containing k sampled values and a consecutive measurement x_m also containing k sampled values. The consecutive measurement x_m is then shifted with respect to the first measurement using the index n.

$$R_{xy}(n) = \sum_{m=0}^{k} x_{m+n} y_m^* \tag{3}$$

Because both signals have nearly the same shape, but are shifted in time, the function delivers a maximum, when both of them are aligned. The corresponding index n of the shift then delivers the necessary information to calculate the new start point. In Fig. 9 the histogram of the calculated start points is depicted. Compared to the results of the previous algorithms shown in Fig. 8 it is clearly visible that the indices are more concentrated between the index 150 and 160, with a distinct peak at 155.

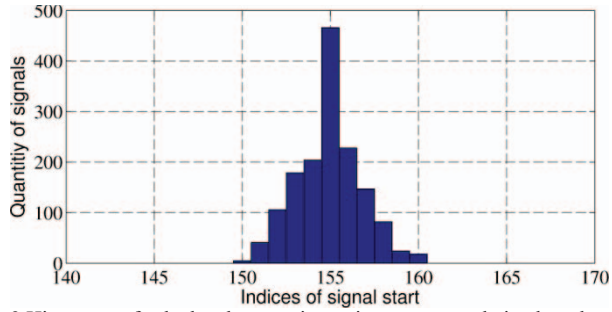

Fig. 9 Histogram of calculated start points using cross-correlation based trigger algorithm

The algorithm thus delivers more accurate values of the start point than the algorithm described before. The characteristics of the algorithm are:

- High usage of hardware resources for longer signal parts
- No causal behavior
- Robust against noisy signals

Because the cross-correlation is a non-causal function, it is not suitable for a real-time implementation. With a causal behavior, there is no dependence on further sample points for the implemented algorithm. With the fulfillment of causality, the algorithm could perform the calculation from sample point to sample point and no further information or memory was needed for the decision process. As real time applicability is very important, a third alternative trigger detection algorithm is also tested.

➢ *Trigger calculation based on averaging with exponential smoothing*

With the target of an implementation on a FPGA, that obtains the data from an ADC unit and processes it within a specific tick count, the constraint for the algorithm is given that no future signal data points are available and the signal start point is determined based on the actual sampled data only. Additionally, the algorithm should be resistant against noisy data. The basic idea is the generation of smoothed signals. Exponential smoothing assigns exponentially decreasing weights over time. Assuming the data samples $y[1],\ldots,y[n]$ with the actual k-th sampled data are given. For the estimation of the signal start point two variables are calculated. First the

smoothed signal is calculated for the measured data (variable denoted with *mean*) with equation (4).

$$mean[k] = \alpha_1 * y[k] + (1 - \alpha_1) * mean[k-1] \quad (4)$$

By direct substitution back into itself the smoothed estimated value $mean[k]$ is calculated with the smooth factor α_1, with $0 < \alpha_1 < 1$. At $\alpha_1 = 1$, no smoothing occurs and with $\alpha_1 = 0$ the smoothed estimated value is used. With $\alpha_1 < 1$, the previous values before the current value $y[k]$ are assigned a lower weight. The second variable (variable denoted with *noiselevel*) is calculated with the absolute value of the difference between actual measured value and smoothed measured data (*mean*) weighted with the parameter α_2, see equation (5).

$$noiselevel[k] = \alpha_2 * abs|y[k] - mean[k]| + (1 - \alpha_2) * noiselevel[k\text{-}1] \quad (5)$$

The trigger is detected when the following condition (6)

$$|y[k] - mean[k]| > c * noiselevel[k] \quad (6)$$

is fulfilled. Beside the parameter for the smooth process (α_1, α_2), the parameter c serves as a kind of threshold and has to be configured manually.

In Fig. 10 the histogram of the trigger indices for the start point found with the new algorithms are shown.

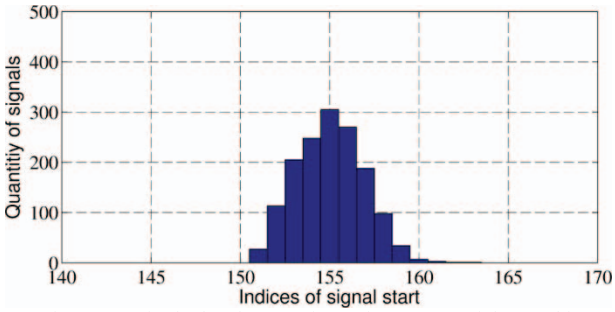

Fig. 10 Histogram of calculated start points using exponential smoothing based trigger algorithm

For the last proposed algorithm the characteristics can be described with

- Low storage and processing overhead needed
- A causal algorithm suitable for real time applications
- Manual tuning of parameter values necessary

In Fig. 11 the influence of an inaccurate trigger detection

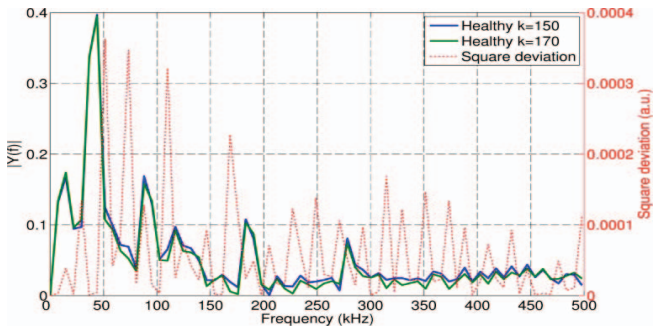

Fig. 11 Comparison between two spectra calculated out of respectively one time signal with inaccurate detection of start points

algorithm is shown with a comparison between a spectrum calculated out of a time signal with start point k=150 (blue trace) and a start point k=170 (green trace). The difference between the two traces is not negligible and a wrong detected start point influences the accuracy of the proposed insulation state detection method (see also Fig. 5).

III. Conclusion

A method to detect insulation degradation based only on the information of two current sensors has been presented. The proposed technique is based on excitation of the machine by voltage steps initiated by the inverter and evaluating the transients of the current sensors. These transients are mainly influenced by the drive's parasitic capacitive components. Insulation degradation is always linked with a change of capacitance that is considered one of the dominant parameters for insulation health state evaluation. A new fault indicator was derived and its sensitivity to changes of the capacitance verified. A combination of four different voltage steps and measurement sequences enables the monitoring of the non-measured phase. There is no significant deterioration of sensitivity if one single phase current sensor is omitted. As the new detection algorithm is sensitive to variations of the signal starting point, three different trigger detection algorithms are tested and compared and an accurate algorithm suitable for implementation in a FPGA is proposed.

Acknowledgment

The work to this investigation was supported by the FFG.
The authors also want to thank National Instruments for the generous support.

References

[1] IEEE Committee Report; "Report of large motor reliability survey of industrial and commercial installation, Part I," I*EEE Transactions on Industry Applications*, vol.21, no.4, pp.853–864, 1985

[2] IEEE Committee Report; "Report of large motor reliability survey of industrial and commercial installation, Part II," *IEEE Transactions on Industry Applications,* vol.21, no.4, pp.865–872, 1985

[3] Kim, H.D.; Yang, J; Cho, J.; Lee, S.B.; Yoo, J.-Y.; "An Advanced Stator Winding Insulation Quality Assessment Technique for Inverter-Fed Machines," *IEEE Trans. on Ind. Appl.*, vol.44, no.2, pp.555-564, (Mar./Apr. 2008)

[4] G. C. Stone, E. E. Boulter, I. Culbert, and H. Dhirani, "Electrical Insulation for Rotating Machines". *IEEE Press*, 2004

[5] Farahani, M.; Borsi, H.; Gockenbach, E.; "Study of capacitance and dissipation factor tip-up to evaluate the condition of insulating systems for high voltage rotating machines," *Electrical Engineering*, vol.89, no.4, pp.263-270, 2007

[6] Perisse, F.; Werynski, P.; Roger, D., "A New Method for AC Machine Turn Insulation Diagnostic Based on High Frequency Resonances," *Dielectrics and Electrical Insulation, IEEE Transactions on* , vol.14, no.5, pp.1308,1315, October 2007

[7] Peroutka, Z., "Requirements for insulation system of motors fed by modern voltage source converters," *Power Electronics Specialists Conference, 2004. PESC 04. 2004 IEEE 35th Annual* , vol.6, no., pp.4383,4389 Vol.6, 20-25 June 2004

[8] Nussbaumer, P.; Santin, C.; Wolbank, T.M.; "Analysis of current reaction on inverter-switching to detect changes in electrical machine's high-frequency behavior," *38th Annual Conference on IEEE Industrial Electronics Society, IECON*, pp.1678-1683, 2012